Lock-in thermography to detect delamination in CFRP

Carosena Meola[1*], Giovanni M. Carlomagno[1], Daniele Annicchiarico[2], Mauro Zarrelli[2] and Michele Giordano[2]

[1]Department of Aerospace Engineering (DIAS), University of Naples Federico II,
Via Claudio, 21, 80125 Napoli, ITALY

[2]IMCB- Institute of Composite Materials and Biomedical CNR- National Research Council
Piazzale Enrico Fermi,1 Portici, Napoli, Italy

ABSTRACT

This paper is focused on testing and evaluation of CFRP specimens with lock-in thermography. Several specimens were prepared with the infusion technique; delamination was simulated with thin Kapton diskettes, which were positioned at given depths through the thickness. Thermal analysis (DSC) and rheological tests were performed in order to achieve the optimal state of the resin both for the infusion process and for the later solidification phase. Artificial defects in the form of thin kapton foils of different shape (circular, elliptical), and dimensions were introduced in each sample. Such inserts were located at different depths and in some cases, by overlapping more than one kapton shaped layer; e.g., two or more concentric disks, each of them with different diameter. Non destructive tests were performed with optical lock-in thermography (OLT) and results were presented in terms of phase angle. All inserts were discovered including information about their shape, dimension and location inside each specimen.

INTRODUCTION

The wide use of carbon fibre reinforced polymer (CFRP) composites [1-2] for primary and secondary structures in the aerospace field is driving the attention of many research groups in developing and testing reliable non-destructive methodologies to asses the structural integrity of these materials [3-11]. In fact, CFRP offer many advantages mainly in terms of strength and lightness, but are susceptible to internal flaws which may arise during manufacture and in service.

Indeed, delamination is one of the most recurrent defects which can be encountered in fibre reinforced materials not only associated to in-service loads but also induced by incorrect or accidental manufacturing stages. These types of material defects are often very light and difficult to be detected with non destructive inspection, although its detrimental effects could lead to final component discharge or ultimately to catastrophic consequences of the real part. For these reasons, the availability of effective NDE techniques [3-10] able to detect delaminations at an incipient stage, is a primary requirement for the reliable design of aerospace composite structures.

The present investigation is focused on the use of optical lock-in thermography (OLT) as suitable technique to detect delamination in composites.

Materials

Specimens were fabricated of two different staking sequences $[45/0/90/-45/+45/0/90/-45]_S$ and $[0,90]_{4S}$ from RTM6 epoxy resin reinforced with G1157 UD 6k carbon fibres by the vacuum infusion process (VIP). Within this technique, fibers are laid dry into the mold; then, vacuum is applied to drive resin. More specifically, once complete vacuum is achieved, resin is literally sucked into the laminate via carefully placed tubing. The

* Corresponding Author: Dr. Carosena Meola
Department of Aerospace Engineering (DIAS)
University of Naples Federico II
Via Claudio 21, 80125 Napoli, ITALY
e-mail: carmeola@unina.it

infusion process is sketched in Fig. 1. This process was chosen because it provides some improvements over traditionally vacuum bagged parts mainly better fiber-to-resin ratio, less wasted resin, very consistent resin usage, unlimited set-up time, cleaner manufacturing.

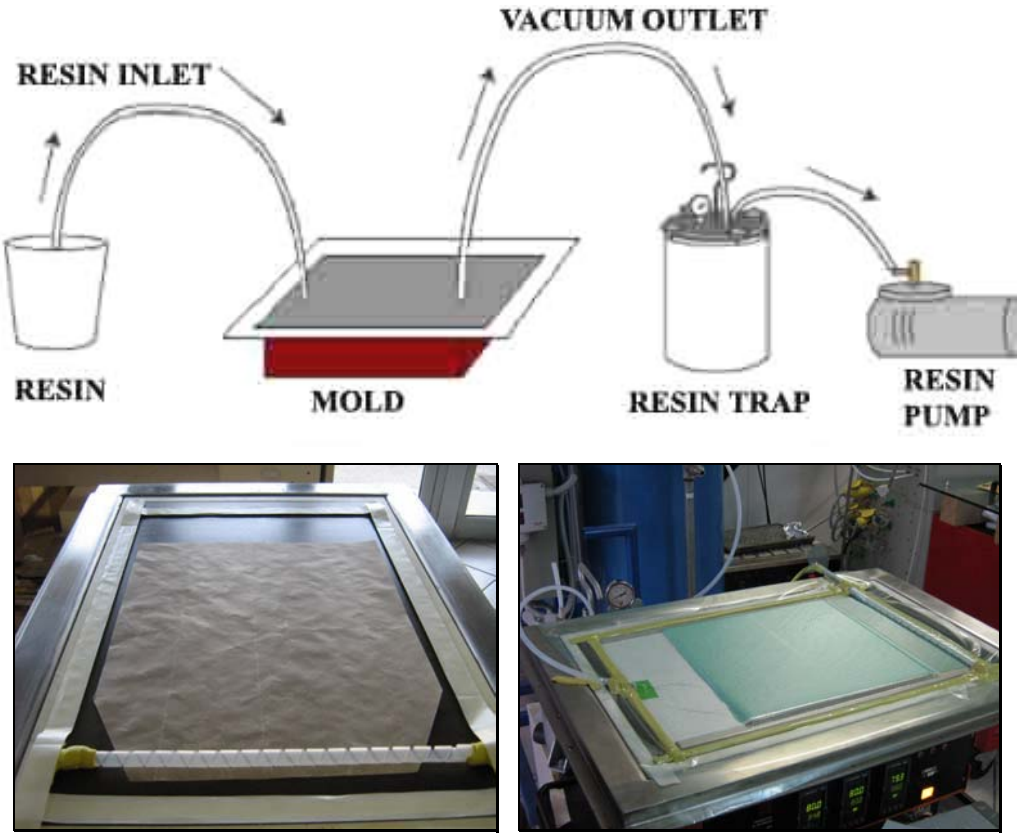

Fig. 1 Scheme of the vacuum infusion process

Preliminary thermal analysis (DSC) and rheological tests were performed in order to achieve the optimal state of the resin both for the infusion process and for the later solidification phase. According to RTM6 data sheet, curing process is 160°C for 1h30 and 180°C for 2h. For DSC characterization, realized with the TA2920 DSC instrument, the normal procedure is to operate at constant temperature rate (Fig. 2) and at isothermal condition (Fig. 3). Dynamic and isothermal data analysis for RTM6 made it possible to make some considerations :

- Dynamic measurement (Fig. 2) present a reticolation peak temperature of 241 °C and energy associated with the reaction of 470 J/g.
- By isothermal analysis, it appears that at 160°C resin time curing is 90 minutes (Fig. 3, green line): relative percentage of cross-link is equal to 83% . The percentage of cross-link is the ratio between area of isothermal curve at 160°C and area of dynamic curve at 10°C/min (Fig. 2, red line).
- For a complete cross-linking, it is necessary a next step of treatment at a temperature greater than 160°C but not exceeding the value of the glass transition temperature, which is equal to 196°C.
- The isothermal temperature for the second step of cure is 180°C: the time of curing at this temperature is sufficiently slow to allow the molecules to rearrange into the matrix for complete cross-linked reaction

Results of rheological characterization (Anton Paar Physica MCR301) permits to identify the optimal infusion temperature. Then, the resin temperature is set at 90°C / 100°C; in this range the viscosity is sufficiently low to allow the resin to flow and distribute inside the layers. The rheological test output is reported in Fig. 4 with the thermal cycle data collected in Errore. L'origine riferimento non è stata trovata..

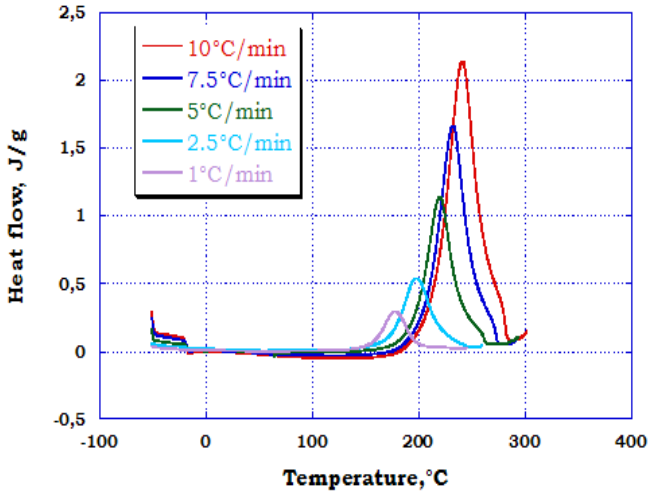

Fig. 2 DSC in constant temperature rate

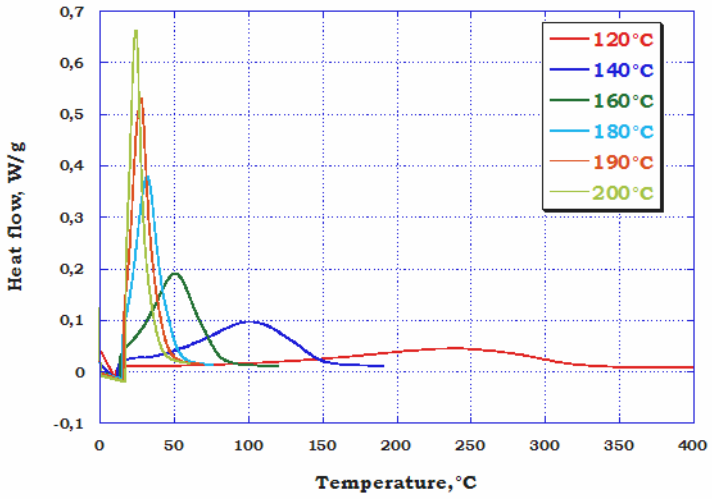

Fig. 3 DSC in isothermal condition

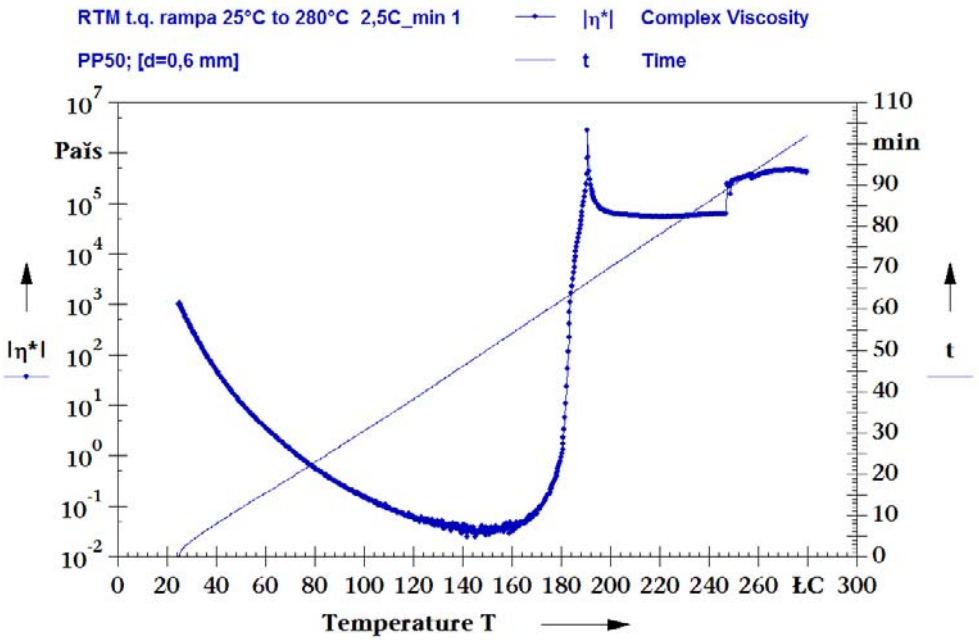

Fig. 4 - Rheological test output

Temperature range [°C]	Thermal rate [°C/min]	Hold time (min)
25°C to 280°C	2.5	-

Table 1 Thermal cycle data for rheological test

Delamination was simulated by inserting thin kapton foils of different shape (circular, elliptical), and dimensions. Inserts were located at different depths and in some cases, by overlapping more than one kapton shaped layer; e.g., two or more concentric disks of different diameter. Owing to the staking sequence, two types of specimens were analysed type I ($[45/0/90/-45/+45/0/90/-45]_S$) and type II ($[0,90]_{4S}$).

Three specimens belong to the type I, which are respectively named I-1, I-2 and I-3. More specifically, I-3 does not include any delamination, while the other two respectively include an insert 140 mm in diameter positioned at 0.5 mm (I-1) and at 0.75 mm (I-2).

Three specimens belong to the type II, which are named P1, P2 and P3 and are represented in details in the following figures 6, 7 and 8. As can be seen, P1 and P2 include circular and elliptical inserts at depth of 0.5 and of 0.75 mm, while the last specimen P3 contains overlapped concentric inserts of increasing diameter moving from 0.5 mm up to 3 mm depth.

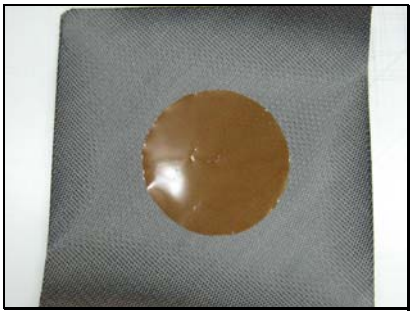

Fig. 5 Cut view of a specimen type I

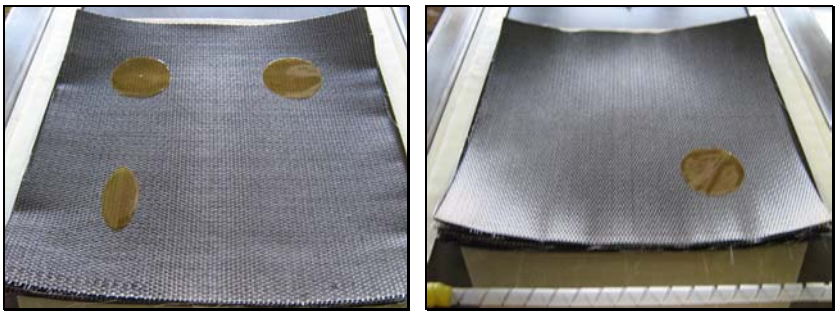

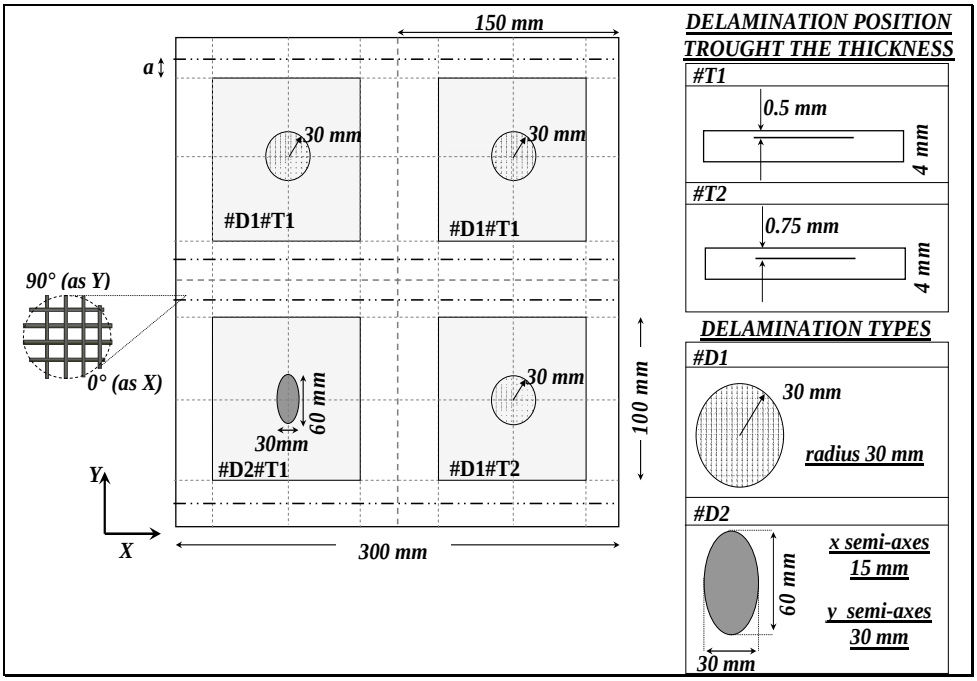

Fig. 6 Representation of the specimen P1

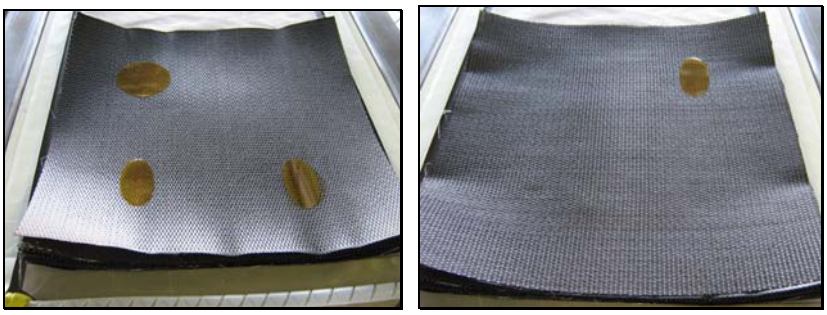

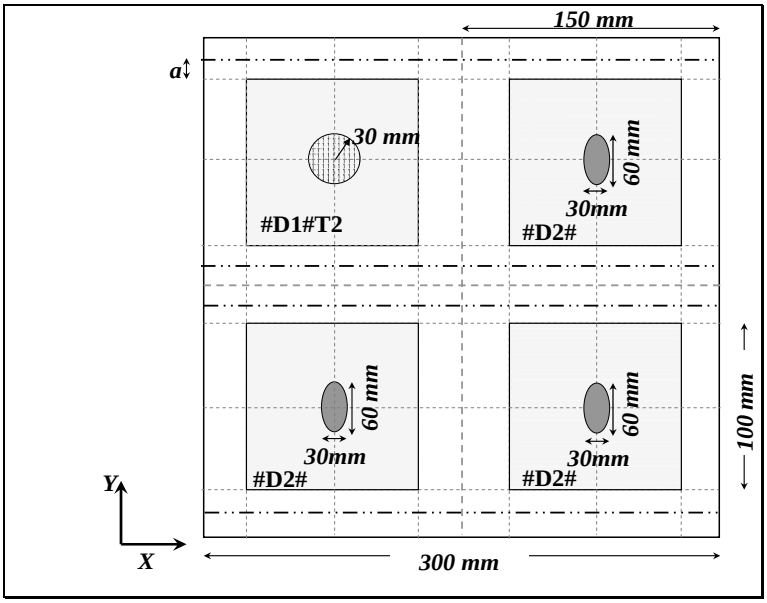

Fig. 7 Representation of the specimen P2

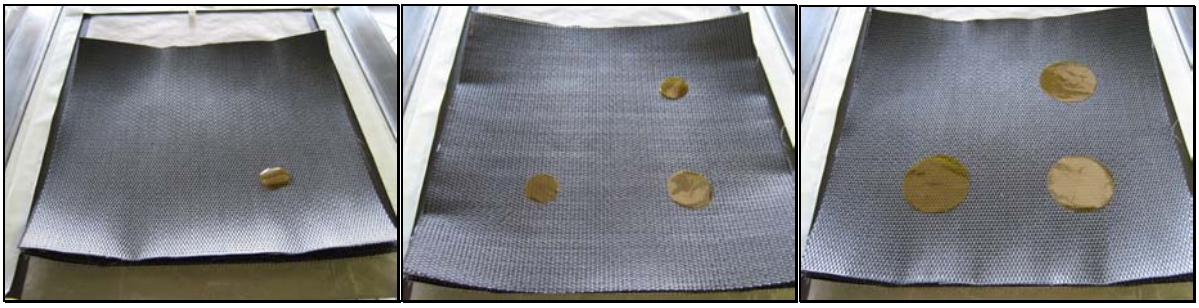

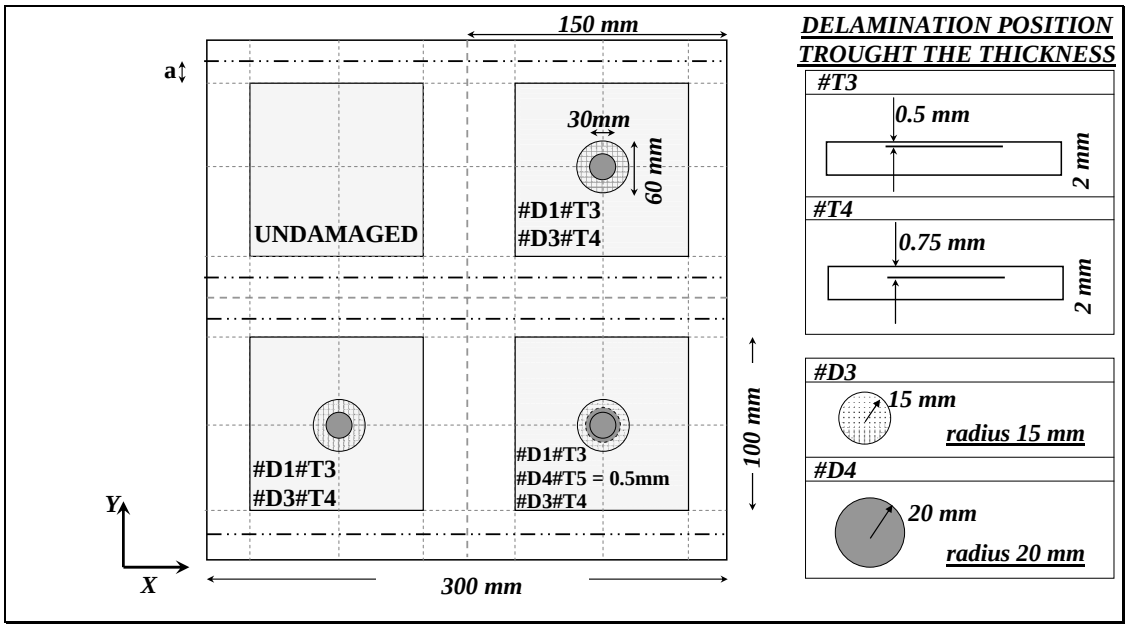

Fig. 7 - Representation of the specimen P3

Non Destructive Evaluation with Lock-in thermography

All the specimens described in the previous section were non destructively evaluated with lock-in thermography to ascertain the correct position of the inserts.

The infrared system

The setup for non destructive tests (NDT) is sketched in Fig.9.

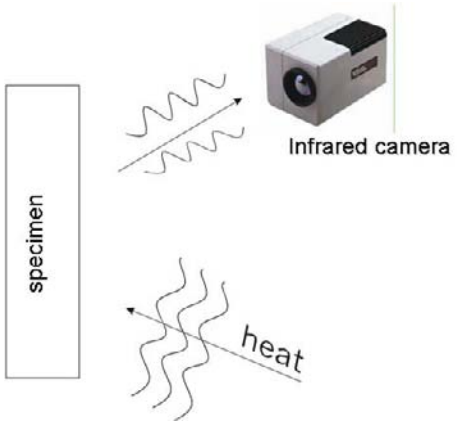

Fig.9 Lock-in thermography setup

The infrared camera is the ThermaCam SC3000 (FLIR Systems), which is equipped with a Stirling cooled Focal Plane Array (FPA) Quantum Well (QWIP) detector working in the Long Wave infrared band 8-9 μm. The sensitivity is 20 mK at ambient temperature allowing for detection of small temperature variations over the specimen surface. The standard acquisition rate is 60 Hz full frame, but it can reach up 900 Hz with a reduced field of view. For non destructive test purposes the infrared camera is equipped with the IRLockIn 4 option and with halogen lamps. With the IRLockIn© software it is possible to select the measure parameters (heat modulation function, frequency and acquisition rate) as well as the image processing method (Fast Fourier, Harmonic Approximation, etc.) and the analysis parameters (number of images, first image in the sequence to be analysed, etc.).

Test procedure

Tests were performed with optical lock-in thermography OLT [5, 8]. More specifically, the thermal energy, generated by halogen lamps, is delivered to the object surface in the form of periodic thermal waves; such waves propagate inside the material and undergo reflections at boundaries. The temperature modulation at the surface is modified by the thermal waves coming back from the inside of the component; an oscillating interference pattern is produced that is captured by the infrared camera. Phase and amplitude of these waves supply information on hindered defects. Both lamps and camera are positioned on the same side with respect to the object. The depth range, for the amplitude image, is given by the thermal diffusion length μ which is calculated from the thermal diffusivity α and the wave frequency *f* :

$$\mu = \sqrt{\frac{\alpha}{\pi f}} \qquad (1)$$

while the maximum depth *p*, which can be reached for the phase image, corresponds to 1.8μ [6-9]. The material thickness, which can be inspected, depends on the wave period (the longer the period, the deeper the penetration) and on the material properties (thermal conductivity, heat capacity and density). Generally, tests start at a quite high wave frequency, at which only surface (or shallow) defects are visible, and later on, to inspect deeper layers, the frequency is decreased until the entire thickness has been traversed.

Results may be presented as phase, or amplitude images; in general, the phase image is preferable because of its insensitivity to non uniform heating and to local variation of emissivity over the surface. In the phase image, a local variation of colour indicates a local variation of phase angle ϕ and, in turn, a local variation of material properties [10].

Results and discussion

In this work, tests were performed with OLT by varying the lamp modulation frequency from 1.75 down to 0.05 ; results are presented as phase images.

<u>Specimens type I</u>

In Fig. 10 are shown some phase images of the type-I specimens. More specifically, the first two images (Figs. 10 a and b), which refer respectively to the specimens 1 and 2, were taken at the same frequency of 0.85 Hz. As can be seen the insert, which is located at 0.75 mm, in the specimen 1 is well outlined, while the insert in the second specimen being deeper, appears at the lower frequency of 0.25 Hz (Fig. 10c). The phase image of the specimen 3 without insert displays only small variations, which may be due mainly to a non perfectly uniform adhesive distribution.

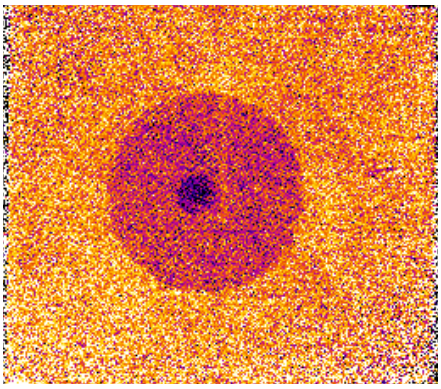

a) I -1 f = 0.85 Hz

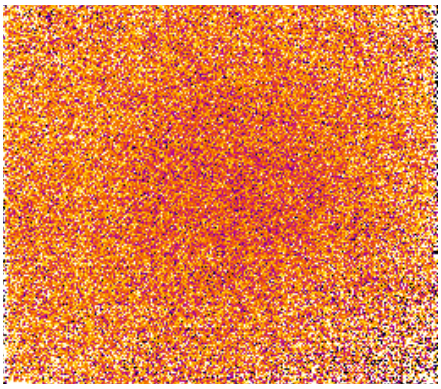

b) I -2 f = 0.85 Hz

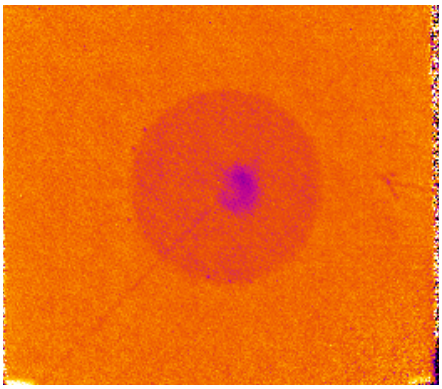

c) I -2 f = 0.25Hz

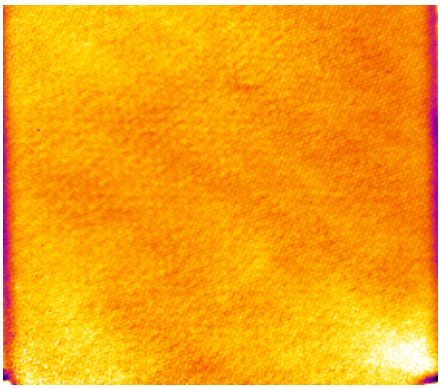

d) I - 3 f = 0.05 Hz

Fig.10 Phase images of type-I specimens

Specimens type II

The specimens P1, P2 and P3 were tested at heating frequencies from 1.5 down to 0.05 Hz; some phase images are reported in the following figures 11-14. As a general comment, all the inserts are detected. In particular, by varying the frequency from 0.5 to 0.25 and to 0.05 (Figs. 13a, b and c) it is possible to visualize first the smaller and shallow inserts at 0.5 mm, then the larger and deeper ones, which are located at 0.75 mm. It is possible to discriminate between the different inserts; to better outile the overlapped diskettes some tests were repeated with close-up view. The images taken with close up view confirm the already noted features and better evidence the eccentricity of the overlapped foils. It has to be noted that the darker zones at the bottom on left and on right (i.e., Figs 11, 12 and 13 a, b) do not indicate presence of anomalies; they are the fixtures to maintain the specimen in vertical position.

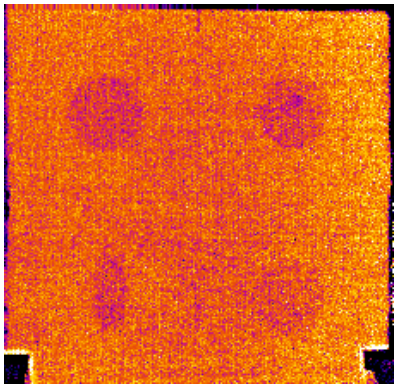

Fig.11 Phase image of the P1 specimen taken at f = 0.5 Hz

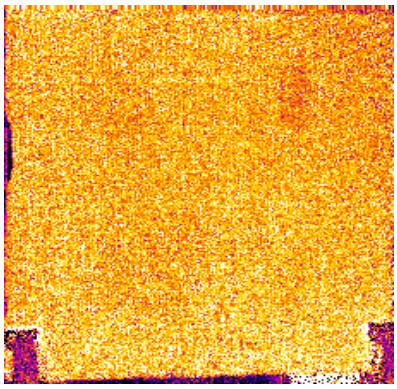

a) f = 1 Hz

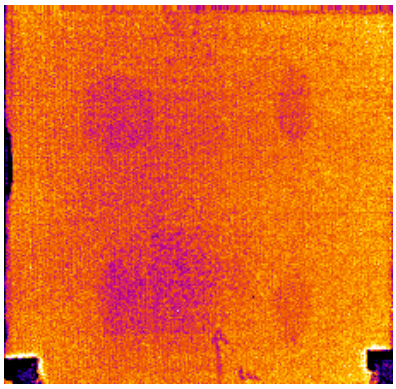

b) f = 0.5 Hz

Fig.12 Phase images of the P2 specimen

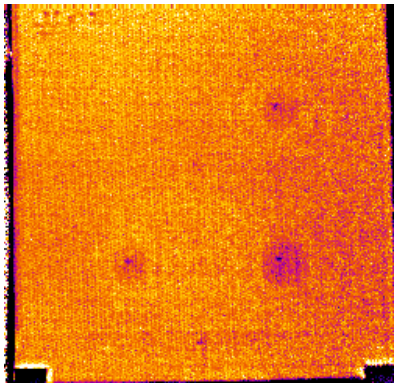

a) f = 0.5 Hz

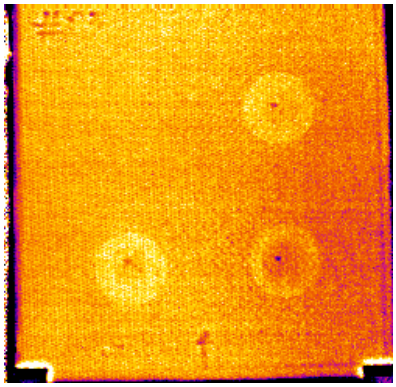

b) f = 0.25 Hz

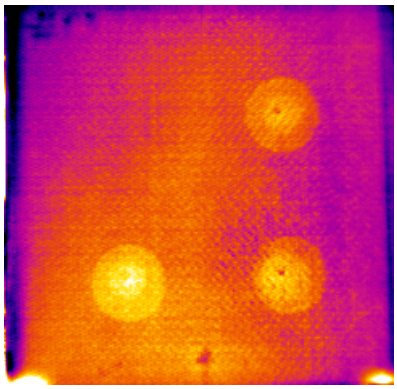

c) f = 0.05 Hz

Fig.13 Phase images of the P3 specimen

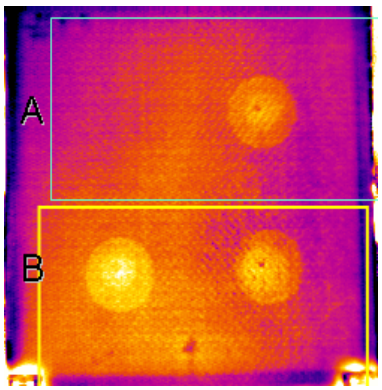

a) phase image of the specimen P3 taken at f = 0.05 Hz

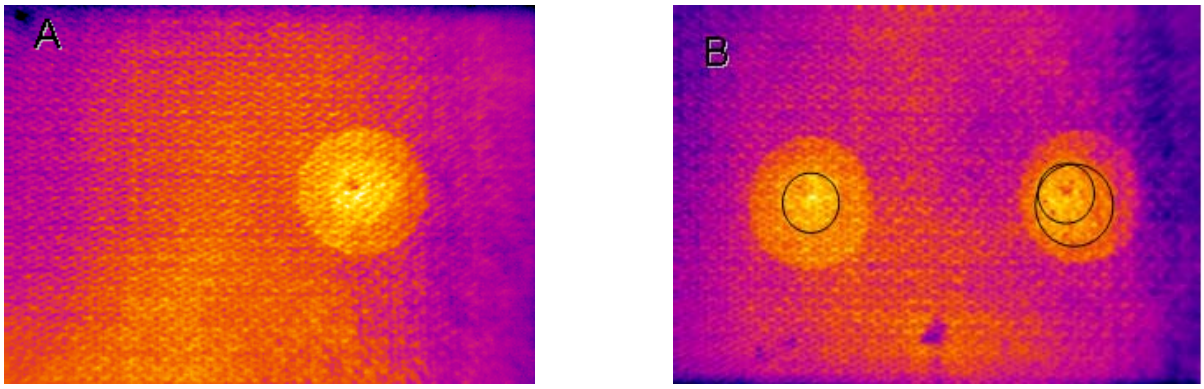

b) close up view of zone A c) close up view of zone B

Fig.14 Phase images of the P3 specimen

CONCLUSIONS

Several CFRP specimens with enclosed kapton inserts, to simulate delaminations, were inspected with optical lock-in thermography. All the inserts were discovered and well outlined; indeed, lock-in thermography allows discrimination of even superimposed foils. In addition to the induced defects, it is also possible to detect imperfections due to manufacturing, such as the eccentricity of some overlapped foils as it is possible to see from Fig. 14c.

REFERENCES

[1] R.M. Jones, Mechanics of composite materials, Hemisphere Publishing Corporation, New York, 1975.
[2] D. Hull and T.W. Clyne, An introduction to composite materials, Cambridge University Press 1996.
[3] Baldev Raj, T. Jayakumar, B.P.C. Rao, Review of NDT techniques for structural integrity, Sadhana, Indian Academy Proc. in Engineering Sciences, Vol. 20, pp. 5-38, 1995.
[4] B.P.C. Rao, Visual Techniques in Non-destructive Testing, Encyclopedia of Materials: Science and Technology, Elsevier Science Ltd, pp 6043-6046, 2001.
[5] A. Dillenz, T. Zweschper, G. Riegert, G. Busse, *Review of Scientific Instruments* Vol. 74, pp. 417-419, 2003.
[6] A. Letho, J. Jaarinen, T. Tiusanen, M. Jokinen, and M. Luukkala, *Electr. Lett.* Vol. 17, pp. 364-365, 1981.
[7] C.A. Bennett Jr. and R.R. Patty, Thermal wave interferometry: A potential application of the photoacoustic effect, *Appl. Opt.* Vol. 21, pp. 49-54, 1982.
[8] G. Busse, *Appl. Phys. Lett.* Vol. 35, pp. 759-760, 1979.
[9] R.L. Thomas, J.J. Pouch, Y. H. Wong, L. D. Favro, P. K. Kuo and A. Rosencwaig, *J. Appl. Phys.* Vol. 51, pp. 1152-1156, 1980.
[10] C. Meola, G.M. Carlomagno, L. Giorleo, *J. Mater. Proc. Technol.* vol.156, pp. 1132-1137, 2004.
[11] C. Meola, G.M. Carlomagno, *J. Adhesion Sci. Technol.* 20, pp. 589-632, 2006.